Macromolecules **2006,** *39,* 9621−9629

Collapse Transition in Random Copolymer Solutions

Ashok Kumar Dasmahapatra[†]

Polymer Science and Engineering Division, National Chemical Laboratory, Pune 411008, India, and Department of Chemical Engineering, Indian Institute of Technology Bombay, Powai, Mumbai 400076, India

Guruswamy Kumaraswamy*[,†]

Polymer Science and Engineering Division, National Chemical Laboratory, Pune 411008, India

Hemant Nanavati*[,†,‡]

Department of Chemical Engineering, Indian Institute of Technology Bombay, Mumbai 400076, India

Received May 6, 2006; Revised Manuscript Received September 25, 2006

ABSTRACT: We present dynamic Monte Carlo lattice simulations of the coil to globule collapse of single chains of a copolymer comprising monomer units, *m* and *c*, wherein there is a net attractive interaction between *c*-units. As the copolymer is cooled, the solvent quality becomes poorer, and the size of the chain decreases, driven by the net $m-m$ and $c-c$ attractions. The strong $c-c$ attraction increases the overall solvophobicity of the chain relative to a homopolymer and, therefore, copolymers collapse more abruptly and at a higher effective temperature relative to homopolymers. We compare copolymers with homopolymers by rescaling collapse data to the same θ values to account for the effect of overall solvophobicity. This comparison shows that the behavior of copolymers and the corresponding homopolymers is identical as the chain size reduces from high temperatures to the θ value. Beyond θ, copolymers with *c*-content $< \sim 50\%$ collapse more abruptly than either homopolymer, after accounting for the difference in overall solvophobicity. Collapse of copolymers containing higher *c*-content is dominated entirely by the $c-c$ attractions, and these chains behave qualitatively like homopolymers with a higher effective solvophobicity. Analysis of the chain structure during collapse provides a structural reason for the qualitative change in copolymer collapse at low *c*-content. When such copolymers are cooled below θ, the *c*-units rapidly aggregate to form an isotropic, compact core surrounded by an anisotropic solvated shell of *m*-units. The shell densifies as the copolymer is further cooled, but remains anisotropic for the finite chain sizes investigated.

Introduction

Understanding how the solution conformation of a random copolymer changes with solvent conditions is of fundamental interest and has implications for the more complex problem of protein folding.[1−3] In a good solvent, a flexible polymer exists in an expanded coil state that, as the solvent quality becomes poorer, shrinks to an ideal θ condition and finally collapses to a compact globule.[4,5] A comprehensive review of theoretical, simulation, and experimental work on the collapse transition of homo- and copolymers has been recently published by Baysal and Karasz.[6] We will not summarize the extensive literature on coil−globule transitions here; rather, we briefly discuss investigations that probe the steepness of the collapse transition and the intermediate structures that form during collapse.

The nature of the transition from coil to globule depends on the chemical nature of repeat units. For example, theory[7] and simulations[8−10] demonstrate that homopolymers collapse via a smooth second-order transition, while copolymers containing mutually attractive comonomer units collapse abruptly through a first-order transition.[11,12] Experimental studies also indicate that copolymers collapse over a narrower temperature range relative to the corresponding homopolymers.[13,14]

Several reports[15−26] indicate the formation of intermediate states during the collapse of a coil to its final compact globule state. Hu[10] suggests that, prior to the formation of the completely collapsed coil in a homopolymer, “microphase separation” within the chain leads to the formation of a molten globule comprising a dense core surrounded by a shell of incompletely collapsed chains. These results are in accord with experiments on aqueous solutions of poly(*N*-isopropylacrylamide) by Wu and co-workers,[17−21] who have observed the formation of a “crumpled coil” state that further compacts to form a “molten globule” before complete collapse, and with the temperature quench experiments of Chu and co-workers,[15,16] wherein polystyrene (PS) chains have been observed to collapse via the formation of an intermediate “crumpled globule” when solutions in cyclohexane are quenched from the θ temperature. Molecular dynamics simulations also support the picture of a two-stage collapse for flexible homopolymers.[8] Raos and Allegra[25] have suggested that interchain clustering could provide an alternative explanation for the experimental results of Chu and co-workers;[15,16] however, they do not rule out a two-stage collapse.

Intermediate molten or crumpled globule states during collapse of a protein could play an important role in mediating the formation of the final folded “native” globule. Therefore, the intermediate states formed during copolymer collapse have attracted considerable attention.[17−21] The structures formed during copolymer collapse are driven by the interactions between the monomers, comonomers, and solvent. Zhang and co-workers[22] report a two-stage collapse for poly(*N*-isopropylacrylamide-*s*-styrene) in cyclohexane, where the intermediate state

---

* To whom correspondence should be addressed. E-mail: hnanavati@che.iitb.ac.in (H.N.); g.kumaraswamy@ncl.res.in (G.K.). Telephone: 91-22-25767215 (H.N.); 91-20-25902182 (G.K.). Fax: 91-22-25726895 (H.N.); 91-20-25893234 (G.K.).

[†] NCL−IITB Collaborative Group for Copolymers.

[‡] Chemical Engineering, Indian Institute of Technology, Powai, Mumbai 400076, India.

10.1021/ma061017q CCC: $33.50

is an ordered coil resembling a molten globule. Wu and Qiu[21] have reported the formation of a core−shell structure during collapse of poly(*N*-isopropylacrylamide) grafted with poly(ethylene oxide) branches. Molecular dynamics simulations of hydrophobic polymers with hydrophilic branches[24] indicate that the chain microstructure results in the formation of stable, shape-persistent globules with a hydrophobic core surrounded by a hydrophilic shell of the branches. Strong comonomer mutual interactions have been shown to lead to the formation of frustrated, incompletely collapsed structures[11,26] that are strongly influenced by the chain microstructure, viz., the distribution of comonomers in the chain.[11]

Copolymer collapse transitions have been investigated using averages over annealed disorder, especially for the protein folding problem. Pande and co-workers[27] have shown that the validity of the annealed approximation is suspect for folding of short proteins modeled using Dill's HP model.[1] Bastolla and Grassberger[28] show that the annealed approximation, though inexact even for large molecules, provides a useful estimate of the thermodynamics governing collapse in both the high- and low-temperature states. Garel and co-workers[29] have shown that for a statistical hydrophilic−hydrophobic copolymer, annealed and quenched averages predict similar phase behavior, but the former predicts a higher transition temperature than the latter.

Most theories or simulations have addressed the problem of amphiphilic copolymer collapse, wherein like units repel each other while unlike units attract and show a θ transition only above a critical value of chain asymmetry.[30,31] However, a θ transition is always observed for copolymers wherein like units attract each other while unlike units repel.[30] We describe in this paper, dynamic Monte Carlo simulations of the collapse of a random copolymer containing relatively solvophilic monomers (*m*-units) and solvophobic comonomers (*c*-units) (e.g., a copolymer containing polar comonomers in an apolar solvent). We show that the behavior that we observe is not "trivial" or "qualitatively similar to a homopolymer case", as suggested by Ganazzoli,[12] but that it demonstrates an interesting dependence on the chain microstructure. Briefly, we show that copolymers containing a small percentage of solvophobic *c*-units collapse abruptly after the θ point relative to either homopolymer after accounting for the increase in overall solvophobicity. This qualitative change in behavior appears to be linked to the formation of an intermediate core−shell structure with incompletely collapsed *m*-units surrounding a compact core of the mutually attractive *c*-units.

We organize our paper as follows: In the next section, we describe the model and our simulation technique. Then, we describe our results and discuss them in the subsequent section, and finally present brief conclusions.

Model and Simulation Technique

A polymer chain of N units is represented by joining N successive lattice sites on a simple cubic grid of size 64 × 64 × 64 with periodic boundary conditions. Each lattice site is occupied by only one unit (either an *m*-unit or a *c*-unit or a solvent molecule). Copolymer chains are generated as described by Hu and co-workers.[32] While we are interested in the collapse of copolymer containing polar comonomers, we use reactivity ratios for ethylene copolymerization with 1-octene using a vanadium catalyst (*m*-unit and *c*-unit reactivity ratios, $r_m = 24.7$ and $r_c = 0.017$, respectively, taken from ref 28, $r_m r_c = 0.42$). To generate a chain with a *c*-unit mole fraction of x, we calculate the appropriate feed mole ratio,[33] F (by solving $F^2 r_m x + F(2x - 1) + (x - 1)r_c = 0$), and use r_m, r_c, and F to calculate the propagation probabilities for the chain. The *c*-unit sequence in the copolymer is random-to-slightly alternating for these reactivity ratios. For simplicity, we will call these copolymers random. We generate a new chain for each simulation, and each chain so generated represents a particular state of quenched disorder for fixed N and *c*-unit content, x. Thus, the data presented in this paper are averaged over different microstructures, viz., different manifestations of quenched disorder. For example, for $N = 128$, $\lambda = 20$, $x = 12.5\%$, our results represent an average over 20 different chains.

Polymer chains are then equilibrated, via a dynamic Monte Carlo (DMC) algorithm with periodic boundary conditions in a cubic lattice. Our algorithm selects a unit (*m*-unit or *c*-unit) randomly and attempts to move to an unoccupied lattice site among the 26 nearest-neighbor lattice sites (along the lattice grid, along body diagonals, and face diagonals, viz., $6 + 8 + 12 = 26$). Each attempted move is termed one Monte Carlo (MC) move. If a vacant site is found, depending on the position of unit along the backbone chain, our algorithm selects the appropriate microrelaxation move. For example, if the selected unit is terminal, then it will attempt to move either by slithering diffusion[34] or by a single site bond fluctuation[35] (cf. end bond rotation) with equal probability. On the other hand, if the selected unit is a nonterminal one, it will attempt to move by a single site bond fluctuation.[35] If a vacant site is not found, it will be treated as an MC move, and the unchanged conformation is counted again for averaging structural properties. Our algorithm ensures that there is no bond crossing and that no lattice site is occupied by more than one monomer, thus satisfying the excluded volume effect criterion. Violation of volume exclusion criteria leads to the termination of an attempted move and counts as an MC move.

Moves are accepted according to the Metropolis criterion.[36] Thus, the change of energy, ΔE (ΔE is normalized by Boltzmann's constant times absolute temperature, kT), for the MC move is calculated, and the move is accepted if $\exp(-\Delta E) \geq p$, where p is a random number, $0 \leq p \leq 1$, generated by using random number generator, MT19937, developed by Nishimura and Matsumoto.[37] This process is repeated to equilibrate the polymer chain.

Our simulation method is not as efficient as recent sophisticated techniques (such as PERM[38] used for simulating the conformations of an isolated chain; Multicanonical Monte Carlo simulation[39] and expanded ensemble method[40] to study collapse, especially in the low-temperature region where the conformational relaxation is very slow; parallel tempering[41] to speed up the equilibration process, etc.); however, our algorithm can be readily used for simulations of polymer melts, results for which we will describe in future publications.

The change in energy for a single MC move, ΔE, is associated with the net change in nearest neighbor *m*-unit−solvent ($m-s$), *c*-unit−solvent ($c-s$), and *m*-unit−*c*-unit ($m-c$) contacts, ΔN_{ms}, ΔN_{cs}, and ΔN_{mc}, respectively. The exchange energy (normalized by kT) of one *m*-unit−solvent contact, B, represents the net *m*-unit−solvent repulsion and is directly related to the Flory χ parameter.[5] Therefore, an increase in B leads to collapse of a solvated chain to form a compact globule. Similarly, the net *c*-unit−solvent repulsion is given by B_{cs}. In the lattice framework, exchange energies are related to the *m*-unit and *c*-unit interaction energies via the quasichemical approximation, assuming that these interaction energies are pairwise additive.[42] Exchange of *m*-units and *c*-units with solvent during an MC move leads to a net change in the number of $m-c$ contacts. The energy change (normalized by kT) arising from the change of an $m{-}c$ contact is given by B_{mc}. Thus, the total normalized energy change for one MC move, ΔE is given by:

$$\Delta E = \Delta N_{ms} B + \Delta N_{cs} B_{cs} + \Delta N_{mc} B_{mc} \qquad (1)$$

Repulsive interactions between $m{-}s$, $c{-}s$, and $m{-}c$, lead to a net attractive interaction between $m{-}m$ and $c{-}c$. Note that eq 1 reduces to the homopolymer case by setting $B_{cs} = B$ and $B_{mc} = 0$.

Here, because we are simulating the collapse of a model chain representing polar copolymers in nonpolar solvents, we assume that the interaction energies of the solvophobic *c*-unit with the relatively solvophilic *m*-unit is similar to that with the solvent. Thus, we set the *c*-unit−solvent interaction parameter equal to the *c*-unit−*m*-unit interaction parameter, viz., $B_{cs} = B_{mc}$. Further, for convenience, we assume that $B_{cs} = B_{mc} = \lambda B$, where, $\lambda > 1$, represents the enhancement of the net *c*-unit−solvent repulsion relative to the net *m*-unit−solvent repulsion. Therefore, eq 1 can be simplified to:

$$\Delta E = (\Delta N_{ms} + \Delta N_{cs}\lambda + \Delta N_{mc}\lambda)B \qquad (2)$$

We choose values of λ ranging from 10 to 50 and examine the collapse of copolymers containing increasingly solvophobic *c*-units in nonpolar solvent. In this work, we term the units that interact with an interaction parameter of λB as *c*-units, while the other chain units are termed *m*-units. As $\lambda \gg 1$ in our model system, ΔE is dominated by $c{-}c$ contact energy.

For a chain comprising N units, N MC moves represent one MC step. In our work, we calculate mean square end-to-end distance, $\langle R^2\rangle$, and radius of gyration,[10] $\langle R_g^2\rangle$, for each MC step and average these over a large number of MC steps (MCS). When the values of $\langle R^2\rangle$ and $\langle R_g^2\rangle$ do not change appreciably with further MCS, we consider that equilibrium has been reached. As mentioned earlier, $\langle R_g^2\rangle$ values represent averages over quenched disorder. However, we find that, over most of the B-range investigated, the error bars (standard deviation) for $\langle R_g^2\rangle$ are typically of the size of the symbol used to plot the data, and thus, simulations of different chains are quantitatively nearly identical. In the B range between θ and collapse, the error bars are about 15%; this value does not affect any of the trends that we discuss.

We describe the spatial distribution of *c*-units by calculating the radius of gyration of only the *c*-units, $\langle R_{gc}^2\rangle$. Thus, if the *c*-units form a compact aggregate, the *c*-unit radius of gyration is smaller than that of the entire chain.

We have also investigated the evolution of the shape of the polymer chain by calculating the principal components of the shape tensor. The shape tensor S^2 can be written as:

$$S^2 = \begin{bmatrix} S_{xx} & S_{xy} & S_{xz} \\ S_{yx} & S_{yy} & S_{yz} \\ S_{zx} & S_{zy} & S_{zz} \end{bmatrix} \qquad (3)$$

where, $S_{xx} = 1/N\sum_{i=1}^{N}(x_i - x_{\mathrm{cm}})^2$ and $S_{xy} = 1/N\sum_{i=1}^{N}(x_i - x_{\mathrm{cm}})\cdot(y_i - y_{\mathrm{cm}})$, x_i and x_{cm} are the *x*-coordinate of *i*th unit and center of mass, respectively.

The eigenvalues of the shape tensor yield the three principal moments of S and represent the shape of the molecule. The eigenvalues (averaged over a large number of conformations) are represented as $\langle S_i^2\rangle$, where $i = 1$, 2, and 3; the shape factors, $L_i{}^2$, given by the ratios, $\langle S_i^2\rangle/\sum_{i=1}^{3}\langle S_i^2\rangle$, provide information about the shape of the molecule. For an isotropic structure, $L_i^2 = {}^1/_3$.

We begin the simulation by placing a polymer chain on the lattice in a regularly folded state. This initial structure is equilibrated at $B = 0$ (viz., at effectively high temperatures or under athermal conditions) using the DMC algorithm. For an isotropic polymer coil, the ratio of $\langle R^2\rangle$ to $\langle R_g^2\rangle$ is 6. Our simulation data shows that $\langle R^2\rangle/\langle R_g^2\rangle = 6.25 \pm 0.05$, as against 6.3694 ± 0.002 for self-avoiding walk (SAW) polymer chains[43] after equilibration. The polymer solution is then "cooled" to $B = 0.2$, by increasing B (for a homopolymer, the step size is 0.005, while for copolymers, the step size is smaller and depends on λ and x), and the structure of the chain is analyzed after equilibration at each value of B. For chains of size $N = 64$, for example, 4×10^6 MCS have been performed at each cooling step. The first 2×10^6 MCS equilibrate the chain, and the subsequent 2×10^6 MCS have been averaged to calculate $\langle R^2\rangle$, $\langle R_g^2\rangle$, and $\langle S_i^2\rangle$. Larger chain sizes ($N = 128$, 256, and 512) are similarly simulated. However, for larger N, a larger number of MCS are performed at each cooling step. We have investigated the swelling of collapsed chains on heating, viz., we decrease B from 0.195 to 0. The $\langle R_g^2\rangle$ values follow the same trend during heating and cooling, indicating that equilibrium is achieved at each step during our simulations, viz., our simulations represent slow cooling experiments.

Results and Discussion

A. Accounting for the Effect of Overall Solvophobicity on Copolymer Collapse. We have simulated single chain collapse for a series of random copolymers with varying *c*-unit content, x ($x = 0$, 6.25, 12.5, 25, 37.5, 50, 87.5, and 100%, $N = 128$, $\lambda = 20$; Figure 1a) and, with varying λ ($\lambda = 10$, 20, 30, 40, and 50, $N = 128$, $x = 12.5\%$; Figure 1b). With increase in *c*-unit content, the decrease in the size of the copolymer chain occurs at progressively lower values of B (viz., higher effective temperatures), and the transition is more abrupt, viz., the transition takes place over a narrower range of B (Figure 1a). Similarly, with an increase in λ (viz., increased $c{-}c$ attraction), there is an enhanced driving force for copolymer collapse and the chain collapses at lower values of B and over a narrower B range (Figure 1b).

The results in Figure 1a,b (influence of x and λ) clearly indicate that the transition from coil to globule state for a copolymer is mainly driven by $c{-}c$ attraction. Because the *c*-units are more solvophobic compared to *m*-units, an increase in either x or λ leads to an increase in the overall solvophobicity of the copolymer chain. Therefore, the abrupt collapse of copolymers at lower values of B observed in Figure 1a,b is anticipated. However, these data do not differentiate between the effects of overall solvophobicity from those of the copolymer chain microstructure. For example, a polymer containing 100% of the *c*-units should exhibit qualitatively similar collapse behavior to a homopolymer of the *m*-units. Because the effective attraction between units of the homopolymer of *c*-units is λB, a plot of $\langle R_g^2\rangle$ versus B^* ($= \lambda B$, see eq 2) is expected to be identical with the collapse behavior observed for a homopolymer of *m*-units. Therefore, we attempt to separate out the influence of the overall increase in solvophobicity by appropriately rescaling B for each copolymer studied.

We rescale the B axis by matching the θ points for the various copolymers as follows:

$$B^* = (B_\theta^{\mathrm{h}}/B_\theta^{\mathrm{c}})B \qquad (4)$$

where, the scale factor, $B_\theta^{\mathrm{h}}/B_\theta^{\mathrm{c}}$ is the ratio of the θ value of B for the homopolymer to that for the copolymer.

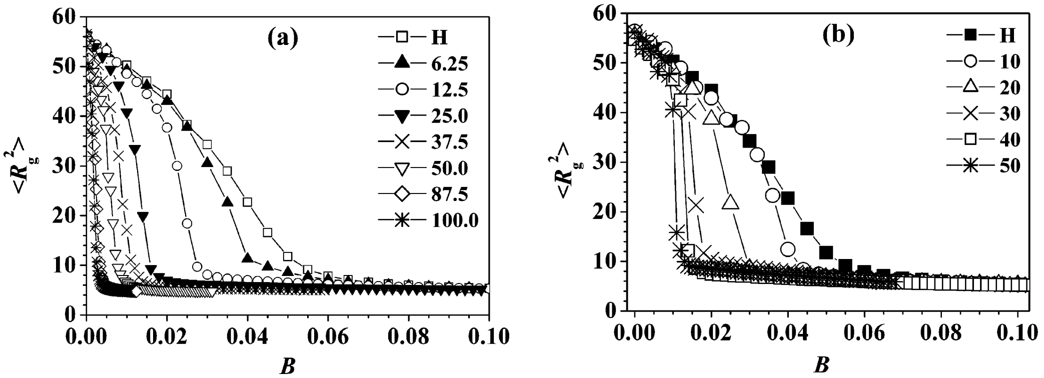

Figure 1. Effect of (a) *c*-unit content, *x* (for $\lambda = 20$), and (b) λ (for $x = 12.5\%$) on collapse of a random copolymer ($N = 128$). H stands for homopolymer. The lines joining the points are meant only as a guide to the eye.

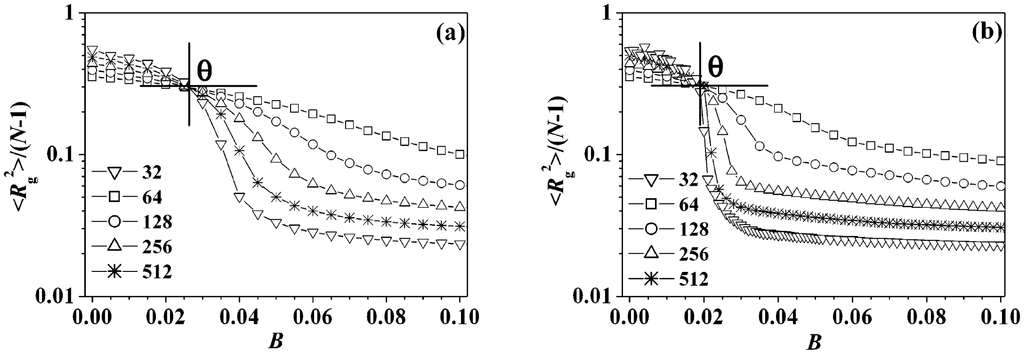

Figure 2. Change in the mean square radius of gyration (scaled by the number of chain segments), $\langle R_g{}^2\rangle/(N - 1)$ as a function of *B* for (a) homopolymer and (b) random copolymer ($x = 12.5\%$, $\lambda = 20$). The θ point is determined at the point where $\langle R_g{}^2\rangle/(N - 1)$ is equal for chains of different length: data for $N = 32$, 64, 128, 256, and 512 are shown as squares, circles, triangles, stars, and inverted triangles, respectively. The lines joining the points are meant only as a guide to the eye. The θ value of *B* is as indicated. Note that the scaled value of the θ chain size is the same for homo- and copolymers.

According to Flory,[5] the θ state is an "ideal" state where the polymer chain is said to attain its unperturbed dimension. At θ, the mean square radius of gyration scales linearly with the chain size $(N - 1)$. Thus, the ratio $\langle R_g^2\rangle/(N - 1)$ is a constant independent of chain length. We use this principle to estimate the θ value of *B* in a manner analogous to Hu:[10] we simulate chains of different length ($N = 32$, 64, 128, 256, and 512) and obtain the θ value as the value of *B* at which $\langle R_g^2\rangle/(N - 1)$ coincides for all *N*. Strictly, a unique θ point is defined only for $N \rightarrow \infty$; for a finite length chain, we obtain instead a "θ region" that approaches the unique θ temperature[44] as $N \rightarrow \infty$. For a homopolymer, we estimate a θ region of $B = 0.027 \pm 0.001$, at which the normalized chain size is $\langle R_g^2\rangle/(N - 1) = 0.29 \pm 0.01$ (Figure 2a). The B_θ and θ value of $\langle R_g^2\rangle/(N - 1)$ obtained here closely match those obtained previously.[10] Similarly, we have calculated the θ region for a copolymer ($\lambda = 20$, $x = 12.5\%$) as $B = 0.019 \pm 0.001$ at which $\langle R_g^2\rangle/(N - 1) = 0.29 \pm 0.01$ (Figure 2b). Because both *m*-units and *c*-units occupy one lattice site in our simulations, the normalized value of the chain coil size, $\langle R_g^2\rangle/(N - 1)$ at the θ region is the same for homo- and copolymers and is equal to 0.29 ± 0.01. We have verified this value of the normalized chain size for copolymers with $x = 6.25$, 25, 37.5, 50, and 87.5% for $\lambda = 20$. Therefore, for the other copolymers, we conveniently estimate the θ region as the *B* value at which $\langle R_g^2\rangle/(N - 1) = 0.29$. We estimate B^* for each of the copolymers mentioned above and present these data in Figure 3. We find that our values closely match with those calculated using the formulation of Chen and co-workers.[45] At low *x* and λ (e.g., $x = 6.25\%$ and $\lambda = 10$) B^* calculated according to the formulation of Chen yields a value of 0.977 *B*, which is aphysical because collapse of a copolymer with attractive comonomer unit cannot take place at effective temperatures that are lower than for the corresponding homopolymer. Our approach, however, does not have this problem and yields values of $B^* > 1$.

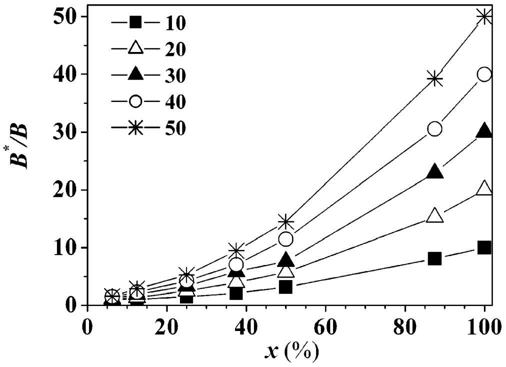

Figure 3. Scale factor, B^*/B for copolymers ($N = 128$) as a function of *c*-unit content for various values of λ. The lines joining the points are meant only as a guide to the eye.

Influence of Copolymer Microstructure. We first investigate the collapse of copolymers with varying comonomer content at $\lambda = 20$, plotted against our rescaled B^* (Figure 4, compare with the data in Figure 1a). Our data demonstrate that the sizes of the copolymer chains are similar in the expanded state ($B^* < B_\theta^*$) and in the collapsed state ($B^* > \sim 0.08$) independent of *x* (Figure 4). The effect of the copolymer microstructure is evident only in a B^* range between the θ region and collapse, where the size of a copolymer deviates from that of the homopolymer. To investigate the effect of the copolymer microstructure at various *x* and λ, we plot the ratio of the size

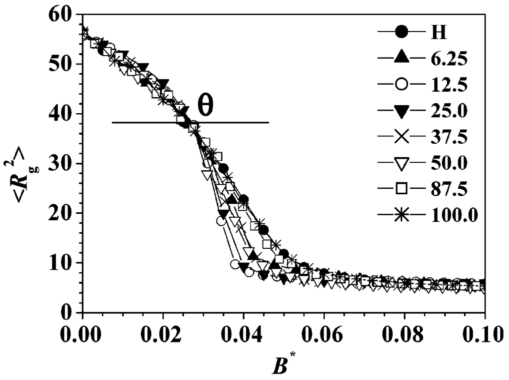

Figure 4. Effect of *c*-unit content on collapse of a random copolymer ($N = 128$, $\lambda = 20$) compared at equal θ by appropriately scaling B^* as described in eq 4. H stands for homopolymer. The lines joining the points are meant only as a guide to the eye.

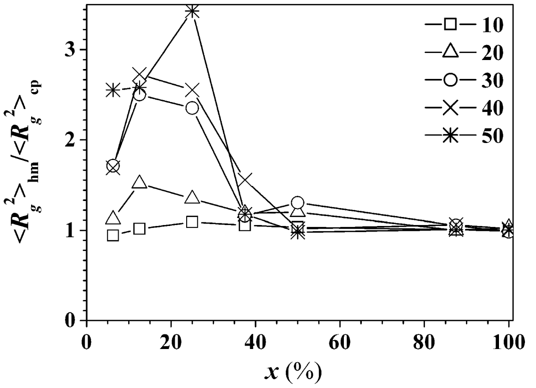

Figure 5. Change in the ratio of mean square radius of gyration of homopolymer to copolymer ($N = 128$) as a function of x at $B^* = 0.034$ for various values of λ. The lines joining the points are meant only as a guide to the eye.

($\langle R_g^2 \rangle$) of the homopolymer to that of the copolymer at $B^* = 0.034$, intermediate between the θ and collapsed states (Figure 5). We have selected this value of B^* arbitrarily, such that the effects of copolymer microstructure are clearly evident. For $x > \sim 50\%$ for all values of λ, the ratio of the size of the homopolymer to that of the copolymer is ~ 1 (Figure 5). For $x < \sim 50\%$ for $\lambda = 10$, this ratio does not deviate much from 1, but for higher values of λ, the deviation is pronounced and reaches a maximum at between 12.5 and 25% for all λ values investigated. Thus, the collapse transition becomes steeper (viz., takes place over a narrower range of B^*) as *c*-unit content increases up to $x = 12.5$ or 25%, depending on the value of λ, and then becomes less steep and is qualitatively similar to homopolymer collapse for values of $x > \sim 50\%$ for the λ values investigated.

As copolymer collapse is driven by the strong attraction between *c*-units, we examine the average number of $c-c$ contacts (*CC*) as a function of x and λ in the expanded coil state ($B^* = 0.01$), in the collapsed state ($B^* = 0.08$), and in the intermediate state ($B^* = 0.034$). In the high-temperature expanded coil state (low B^*), we expect that *CC* should scale as x^2, while in the compact collapsed globule state (high B^*), the *c*-units are expected to be aggregated, and therefore we anticipate that the number of $c-c$ contacts should scale as x (the scaling in the globule state is expected to hold strictly only for globules containing a large number of *c*-units). When we plot the ratio of CC/x as a function of x, at $B^* = 0.01$ for copolymers containing various *c*-unit contents, we observe that this number approximately scales with x, while at $B^* = 0.08$, the CC/x is almost independent of x at higher x (Figure 6). Interestingly, at $B^* = 0.034$, the number of $c-c$ contacts exhibits nonmonotonic behavior in the range of x, where we observe the effects of copolymer microstructure on collapse (Figure 6). This strongly indicates that the rapid collapse in the copolymer size (relative to the homopolymer) that we observe for the copolymers is driven by the formation of a larger than average number of $c-c$ aggregates.

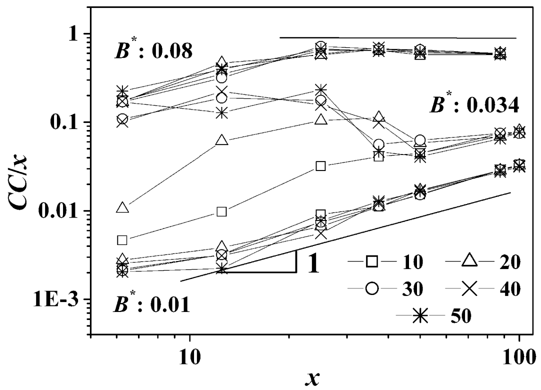

Figure 6. Change in the ratio of number of $c-c$ contacts (*CC*) to *c*-unit content (x) for copolymers ($N = 128$) as a function of *c*-unit content for various values of λ at $B^* = 0.01$ (expanded coil), 0.034 (intermediate between θ and collapse), 0.08 (collapsed globule). A line with slope of 1 is shown near the data for $B^* = 0.01$ as a guide to the eye. The lines joining the points are meant only as a guide to the eye.

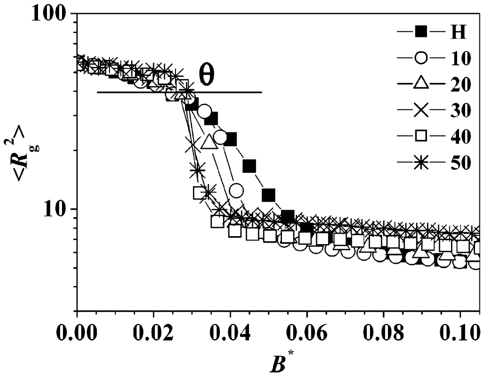

Figure 7. Effect of λ on collapse of a random copolymer ($N = 128$, $x = 12.5\%$). The polymers are compared at equal θ by plotting vs the appropriately scaled B^*. H stands for homopolymer. The lines joining the points are meant only as a guide to the eye.

Before we discuss the implications of these results, we present data for collapse of copolymers containing 12.5% *c*-units as λ is increased from 10 to 20, 30, 40, and 50 ($N = 128$, Figure 7). The sizes of the copolymer chains are plotted versus B^* obtained by rescaling B by B_θ^h/B_θ^c. Again, we find that the collapse is steeper as we go from the homopolymer to copolymers with increasing values of λ. However, for $\lambda > 30$, the initially abrupt decrease in $\langle R_g^2 \rangle$ beyond θ transitions to a slower decrease before a compact globule is formed (Figure 7). For $\lambda = 30$, 40, and 50, the average coil size is higher relative to the homopolymer even at $B^* = 0.1$ where we expect the chains to have completely collapsed. This effect is not an artifact of our simulations because the percentage of accepted MC moves is similar for $\lambda = 20$ and 50 (viz., above and below $\lambda = 30$). Also, we do not observe any hysteresis in the size of the copolymer chain when we reheat and expand collapsed copolymer chains even with $\lambda = 50$. We believe that the large $c-c$ attraction at $\lambda > 30$ may lead to the formation of a *c*-unit aggregate that prevents the chain from contracting rapidly to form a more compact conformation.

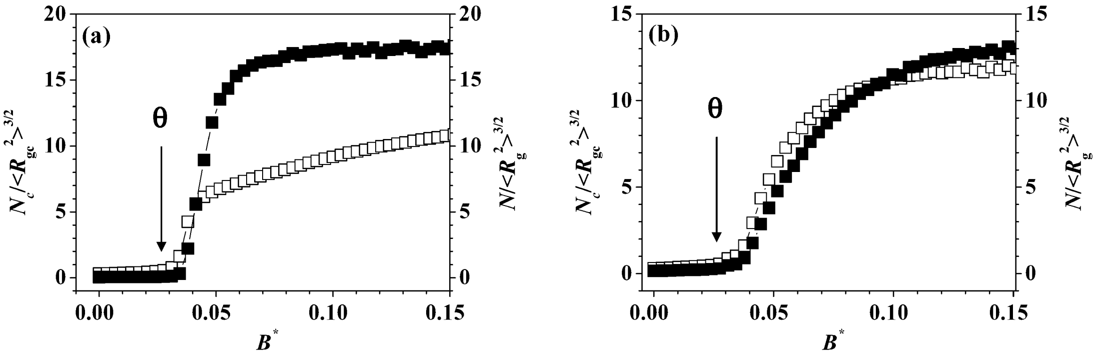

Figure 8. Comparison of the density (as defined in the text) as a function of B^* for a random copolymer $N = 128$, $\lambda = 20$ (a) $x = 12.5\%$, (b) $x = 50\%$. Filled symbols represent the density of the *c*-units, while the empty symbols represent the density of the entire chain. The θ point is as indicated.

Comparison with Literature. Our results accord qualitatively with experimental studies that have observed that copolymers collapse over a narrower temperature interval relative to the corresponding homopolymers (Figure 1). For example, it has been reported that collapse of a copolymer of styrene and methyl methacrylate (MMA) in isoamyl acetate is more abrupt compared to collapse of poly(methyl methacrylate) (PMMA).[14] Also, while polystyrene (PS) has a θ temperature of 18.5 °C in a nonpolar solvent, decalin (cis/trans 60:40), a polar copolymer of polystyrene sulfonic acid (PSSA, with a sulfonation level of 2 mol %) shows a θ temperature of 151 °C.[46] Thus, B^*/B for the pair of PS and PSSA can be calculated as $(T_\theta^{\mathrm{PSSA}}/T_\theta^{\mathrm{PS}}) \sim 1.45$. From Figure 3, we can estimate that this corresponds to a $\lambda \approx 30$ at $x = 2\%$. Thus, it appears that the range of λ values considered in our work is appropriate to model the collapse of copolymers containing polar comonomers (solvophobic *c*-units) in apolar solvents.

Our results also match with the predictions of Ganazzoli,[12] who theoretically showed that copolymers collapse more abruptly as compared to homopolymers, but that, as expected, the behavior of a "copolymer" at $x = 100\%$ is qualitatively similar to that of a homopolymer. Theory indicates that copolymer collapse is a first-order transition while flexible homopolymers collapse through a smooth second-order transition.[7] We do not probe the order of the collapse transition in our simulations; however, the decrease in $\langle R_g^2\rangle$ for the copolymer during collapse is observed to be steeper relative to that for homopolymers (Figure 4), even after accounting for the increase in overall solvophobicity of the copolymers.

Simulations suggest that polymer chains collapse via the formation of an initial dense nucleus surrounded by a partially collapsed chain.[10] Collapse proceeds as this nucleus grows by reeling in chain units. In homopolymers, monomers near the surface of the initial nucleus are reeled in.[2] In copolymers, the initial nucleus is made up of *c*-units and collapse is driven by the net attraction of *c*-units to the nucleus.[2,12] Simulation data suggest that this structural difference underlies the change from second-order collapse in homopolymers to first order in copolymers.[12,26] Our data too suggest a structural origin for the relatively abrupt collapse of copolymers: we observe that values of λ and x that lead to abrupt collapse are related to an increased number of $c-c$ contacts in the intermediate state that precedes the formation of the final collapsed globule (Figure 6). Therefore, we expect that an exploration of the spatial structure of the copolymer chain as it collapses may yield valuable insights into the influence of copolymer microstructure on the collapse transition. This is investigated in the next section.

Structure of the Copolymer Chain during Collapse. In this section, we examine the structure of the copolymer chain as it transitions from an expanded coil at low B^* through the θ condition to the final collapsed globule at high B^*. We focus on a copolymer with $N = 128$, $x = 12.5\%$, and $\lambda = 20$, viz., a copolymer that undergoes an abrupt collapse relative to the corresponding homopolymer and present results for the structure of the chain as the value of B^* is increased.

A comparison between the density of the entire copolymer chain (defined as the number of units, N, divided by $\langle R_g^2\rangle^{3/2}$, a measure of the chain volume) and the density of only the *c*-units (defined as the number of comonomers, N_c, divided by the $\langle R_{gc}^2\rangle^{3/2}$, a measure of the volume occupied by the *c*-units) provides insights into the structure of the copolymer chain as B^* is increased. For B^* below the θ value, *m*-units and *c*-units are distributed equally densely in space (Figure 8a). However, slightly above the θ value of B^*, the *c*-unit density increases abruptly. At this same B^* value, the overall density of the polymer chain also exhibits an equally abrupt but smaller increase. However, while the *c*-unit density plateaus after the abrupt increase, the remainder of the chain continues to densify (Figure 8a). Thus, as B^* increases, the *c*-units aggregate, driven by their strong repulsion for the *m*-units and the solvent. The abrupt increase in the overall chain density observed in Figure 8a is also driven by the formation of this *c*-unit aggregate. It is interesting to compare this behavior with that of a chain with $N = 128$, $x = 50\%$, and $\lambda = 20$ (Figure 8b), viz., a chain that effectively behaves like a homopolymer (Figure 4). For this copolymer, the increase in the density of *c*-units parallels that in the density of the entire chain; beyond the θ point, both densities increase. This densification is rapid initially (but not as rapid as for the low x copolymer) and then continues gradually.

Snapshots of the $x = 12.5\%$ copolymer equilibrated at various B^* values indicate that the chain is expanded at $B^* = 0$ (Figure 9a). At $B^* \sim 0.0276$, near the θ state, *m*-unit and *c*-units stay solvated (Figure 9b). However, at $B^* = 0.041$, above the θ value, the *c*-units collapse to form a dense core that is surrounded by *m*-units that remain solvated (Figure 9c). These *m*-units then begin collapsing (Figure 9d, $B^* = 0.055$) and finally form a dense globule (Figure 9e, $B^* = 0.138$) that retains the *c*-core–*m*-shell structure that originates near the θ state.

Our data demonstrate that copolymer collapse proceeds via a two-stage process, first forming a dense *c*-unit aggregate (the "core"), and subsequently compacting at higher B^* by aggregation of *m*-units. The formation of the core (aggregate of *c*-units) is abrupt and happens at B^* slightly greater than B_θ^*. At θ and for B^* values slightly greater than θ, the *m*-sequences between *c*-units remain solvated around the dense *c*-unit core. This configuration appears to be similar to the "flowerlike" intermediate state that has been recently observed to precede collapse

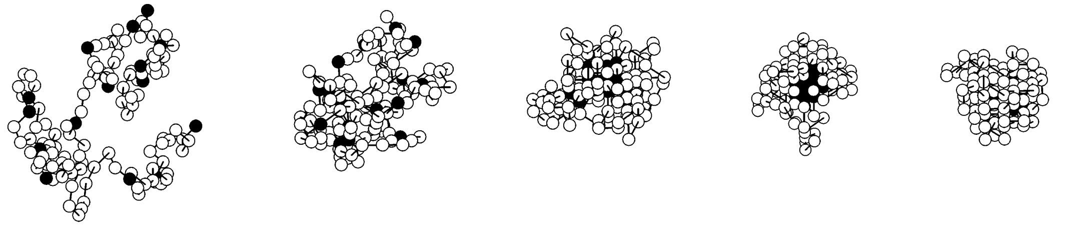
(a) $B^* = 0$ **(b) $B^* = 0.0276$** **(c) $B^* = 0.041$** **(d) $B^* = 0.055$** **(e) $B^* = 0.138$**

Figure 9. Snapshots of the structural evolution a random copolymer chain ($N = 128$, $x = 12.5\%$, $\lambda = 20$) during collapse. *m*-units and *c*-units are represented by empty and filled symbols, respectively. $B^* = 0.0276$ represents the snapshot at θ state.

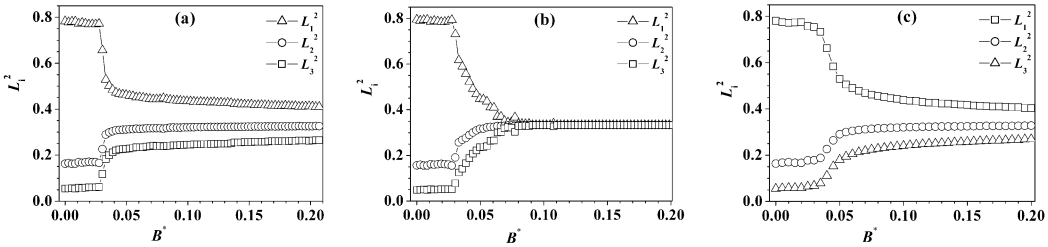

Figure 10. Change in the shape factors as a function of B^* for (a) copolymer ($N = 256$, $x = 12.5\%$, $\lambda = 20$), (b) for the *c*-unit core and (c) for a homopolymer ($N = 256$). The lines joining the points are meant only as a guide to the eye.

in poly(*N*-isopropylacrylamide)−poly(ethylene oxide) graft copolymers.[22] Finally, the shell of *m*-units then collapses slowly around the *c*-unit core to form the final core−shell globular structure.

We analyze the shape of the copolymer chain as it collapses, using the ratio of the eigenvalues (L_i^2) of the shape tensor, S^2. We plot the change of L_i^2 with B^* for the entire copolymer chain ($N = 256$, $\lambda = 20$, $x = 12.5\%$, Figure 10a) for the *c*-units in the same copolymer chain (Figure 10b) and for the corresponding homopolymer ($N = 256$, Figure 10c). In the expanded coil state, homo- and copolymer chains are extended. Topological connectivity of the units along the polymer chain leads to an anisotropic shape with shape factors, L_i^2, in the ratio of 14.1:2.94:1. The shape factors change above B_θ^* and approach each other as the chain begins to collapse (Figure 10a,c). The change in the shape factors is gradual for the homopolymer relative to the copolymer. Even in the collapsed globule state, we observe that L_i^2 are not equal, viz., the globule is not spherical. Rather, we obtain an ellipsoidal core−shell structure with shape factors L_i^2 in the ratio of 1.62:1.25:1 (Figure 10a).

In our simulations, the anisotropy that we observe is affected by the discreteness of the lattice used. However, the final globule is predicted to be anisotropic by molecular dynamics[47] and Monte Carlo simulation[48] studies, even for the case of homopolymer collapse. These values for the copolymer anisotropy from our simulations accord well with homopolymer theory[49] and previous simulations.[48] The shape of the final globule state of copolymer is similar to that of a homopolymer (compare parts a and c of Figure 10). For a copolymer, collapse is mediated by the formation of a core consisting of *c*-units. From the shape factors for only the *c*-units comprising the core, we observe that the compact *c*-unit core is essentially isotropic (Figure 10b). Thus, the picture that emerges is that, during collapse, the *c*-units aggregate to form an isotropic core that is surrounded by incompletely collapsed *m*-units in the copolymer chain. These *m*-units slowly approach an isotropic shape with increase in B^*, but for the B^* values investigated here, the entire chain remains ellipsoidal.

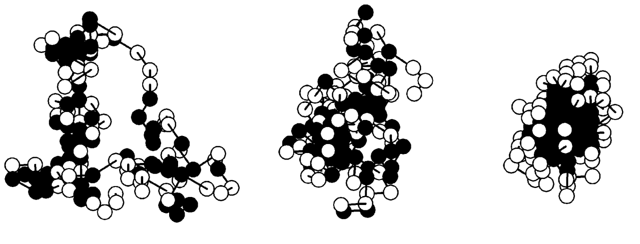
(a) $B^* = 0.034$ **(b) $B^* = 0.041$** **(c) $B^* = 0.11$**

Figure 11. Snapshots of the structural evolution a random copolymer chain ($N = 128$, $x = 50\%$, $\lambda = 20$) during collapse. *m*-units and *c*-units are represented by empty and filled symbols, respectively. $B^* = 0.034$ represents the snapshot at θ state.

Finally, we contrast the behavior observed for the copolymer with $N = 128$, $x = 12.5\%$, and $\lambda = 20$ (Figure 9) with a copolymer chain having a higher *c*-content ($N = 128$, $x = 50\%$, and $\lambda = 20$, Figure 11) that collapses in a manner that is qualitatively similar to homopolymers (see Figure 4). As the chain with higher x is cooled to the θ value, the chain conformation appears similar to that observed for the chain with $x = 12.5\%$ (compare Figure 9b with 11a, B^* values closest to the B_θ^* we selected). When B^* is increased to ∼0.041, in the region between θ and collapse, we observe that unlike the formation of a well-defined core−shell structure in the $x = 12.5\%$ copolymer (Figure 9c), the copolymer with $x = 50\%$ does not exhibit any microphase separation and does not collapse (Figure 11b). The final collapsed state for the polymer with $x = 50\%$ exhibits a core−shell morphology (Figure 11c). However, this structure is not as clearly defined as in the case of the polymer with $x = 12.5\%$ (Figure 9e). These qualitative differences have been illustrated in parts a ($x = 12.5\%$) and b ($x = 50\%$) of Figure 8 for quantitative comparison.

Therefore, it appears that the effect of copolymer microstructure is evident only in cases where the collapse happens via the formation of a well-defined core−shell structure. We note here that we are comparing the spatial structure of copolymers at the same B^*, viz., after accounting for the effect of the overall solvophobicity. For chains with increased x, it appears that the only effect of the *c*-units is to increase the overall solvophobicity, and apart from this, the collapse is qualitatively similar to that of a homopolymer. Hu[10] has claimed that even homopolymer chains exhibit an internal "microphase segrega-

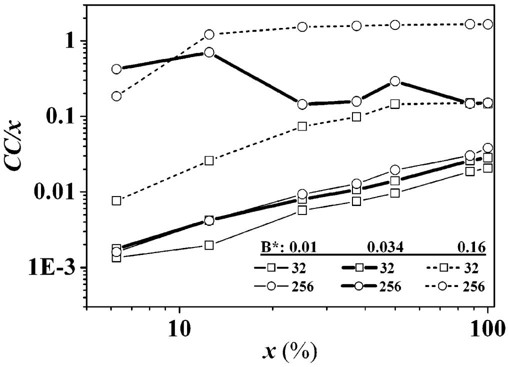

Figure 12. Change in the value of CC/x for copolymers ($\lambda = 20$) with various chain lengths ($N = 32$ and 256) as a function of x and at $B^* = 0.01$, 0.034, and 0.16. We highlight the data for $B^* = 0.034$ using bold lines. The lines joining the points are meant only as a guide to the eye.

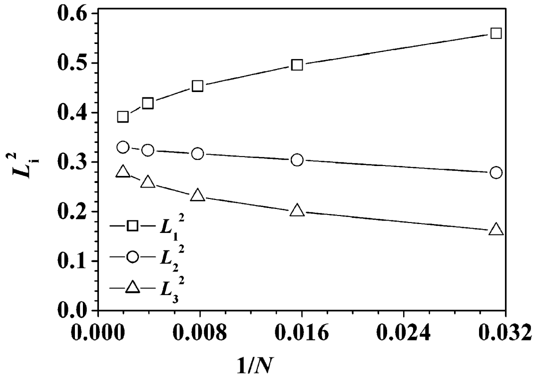

Figure 13. Change in the shape factors as a function of $1/N$ for a random copolymer ($x = 12.5\%$, $\lambda = 20$) for $N = 32$, 64, 128, 256 at $B^* = 0.16$. The lines joining the points are meant only as a guide to the eye.

tion" between a compact core and a disordered, crumpled shell during collapse. In the case of copolymers containing a "small" percent of highly mutually attractive *c*-units, this core−shell microphase separation happens between a compact *c*-unit core and an *m*-unit shell. The formation of this microsegregated structure appears to be responsible for the qualitative change in behavior for copolymer collapse relative to homopolymers. With increase in x or λ, the behavior of the copolymer chain is dominated by the *c*-units. Therefore, these chains simply behave like homopolymers with a higher solvophobicity, and the effect of copolymer chain microstructure is no longer apparent.

Effect of Chain Length. In this last section, we examine the effect of the chain size, N, on copolymer collapse. We have seen that for "small" *c*- content (for example, $x = 12.5\%$ at $N = 128$ and $\lambda = 20$), the *c*-units in the copolymer undergo a microphase separation beyond the θ region and aggregate to form a compact core surrounded by a shell of *m*-units. The formation of this core−shell structure makes the collapse from the θ state more abrupt relative to that for a homopolymer. It is interesting to examine the effect of chain length on microphase separation, viz., on the formation of this core−shell structure. This will provide insight as to whether this microphase separation persists at and influences the "true" phase transition, viz., for chains of infinite N. Our simulation technique limits the chain sizes that we can probe. However, we obtain a qualitative understanding of the effect of chain size by varying N ($N = 32$, 64, 128, and 256). We see that the variation in the number of $c-c$ contacts with x is essentially identical and scales with x^2 for the range of N in the expanded coil state, viz., at $B^* = 0.01$ (Figure 12). For clarity, in Figure 12, we plot only the results for $N = 32$ and 256 and note that the data for the other chain lengths are qualitatively similar. In the collapsed globule state ($B^* = 0.16$; we choose $B^* = 0.16$ rather than 0.08 because chains with $N = 32$ undergo a significant decrease in their size beyond $B^* = 0.08$), the number of $c-c$ contacts increases approximately linearly with x for all N; as the number of *c*-units increases with N, the number of $c-c$ contacts also increases with increasing N (Figure 12). At both $B^* = 0.01$ and 0.16, the increase in the number of $c-c$ contacts is monotonic. However, in the intermediate state between θ and collapse, $B^* = 0.034$, we observe that the number of $c-c$ contacts is nonmonotonic with a higher number of contacts at $x < 50\%$ (Figure 12). As seen previously, this is a signature of the formation of the *c*-unit aggregate core. Therefore, it appears that the effect of copolymer microstructure at *c*-unit content, $x < 50\%$, persists with increase in N. This is strongly indicative that the formation of a *c*-unit aggregate core and *m*-unit shell happens even at larger N and that this microphase segregation leads to a more abrupt collapse transition. This result accords with theoretical predictions of a change in the order of the "true" collapse transition from second order for homopolymers to a steeper first-order transition for copolymers.[12] Our data also suggest that, for higher x, the copolymer behaves essentially like a homopolymer and the order of the phase transition then returns to second order.

Finally, we examine the shape of the collapsed globule at $B^* = 0.16$ (for $N = 32$, 64, 128, 256, and 512). We have observed that the globules are not isotropic (Figure 10a). This is true not only for copolymers but also for homopolymers (Figure 10c). The anisotropy is more pronounced at low N, and the shape factors approach each other as N increases (Figure 13). It appears that at infinite N, the collapsed globule tends to $L_i^2 = {}^1/_3$. We have seen that a copolymer with $N = 256$, $x = 12.5\%$, and $\lambda = 20$ exhibits a core−shell structure with a compact, isotropic core comprising *c*-units surrounded by an ellipsoidal shell of *m*-units (Figure 10). The anisotropy in the overall shape of the copolymer (Figure 13) is similar to that observed for homopolymers and follows the same trend with increasing N, viz., it approaches a more isotropic shape as N increases. Thus, there appears to be no specific role of the copolymer microstructure on the final shape of the collapsed globule, viz., it affects only the "path" between the θ and globule states.

Summary and Conclusions

We describe the collapse of a copolymer chain as it is cooled from an expanded coil state through the θ region to a collapsed globule using dynamic Monte Carlo lattice simulations. The salient features of our investigations are: (1) We model the collapse of copolymers containing solvophobic *c*-units (e.g., polar *c*-units in nonpolar solvents) in a Flory-like approach: (a) We choose a higher penalty for an $m-c$ or a $c-s$ contact relative to an $m-s$ contact. (b) The high effective $c-c$ attraction leads to an increase in the overall solvophobicity of the chain relative to a homopolymer, and therefore, copolymers collapse abruptly and at higher effective temperatures relative to homopolymers.

(2) We compare polymers at the same solvophobicity by rescaling the collapse data so as to match the θ temperatures of these polymers. The rescaled data reveal that: (a) In the high-temperature region from the expanded coil state to θ, enthalpic interactions between chain units are unimportant and homo- and copolymer chains show the same collapse behavior after normalizing (scaling) out the overall solvophobicity. (b) The overall solvophobicity is normalized empirically by rescaling the B axis to make coincident the θ point for the various copolymers. (c) Beyond the θ point, copolymers containing

<50% *c*-units collapse over a narrower region and at higher effective temperatures. (d) Copolymers with higher *c*-content behave in a manner that is qualitatively similar to homopolymers when the overall solvophobicity is normalized.

(3) Our results point to an interesting structural origin to the influence of copolymer chain microstructure on collapse. (a) For copolymers with <50% *c*-units, the *c*-units aggregate due to their strong mutual attraction to form a dense isotropic core as the chain is cooled below θ, thus exhibiting distinct *c*-core–*m*-shell morphology. (b) The anisotropic *m*-unit shell that surrounds the *c*-unit core is "fluffy" and densifies on further cooling. The collapsed core–shell globule is anisotropic, but the anisotropy decreases with increase in chain length. (c) Our data suggest that the aggregation of the comonomers to form a core–shell structure in copolymers containing <50% *c*-units persists as the chain length is increased. (d) Copolymers containing more than 50%, *c*-units are dominated by the mutual attraction of *c*-units and behave essentially like homopolymers having a higher effective solvophobicity. (e) The solvophobicity-normalized copolymer microstructure affects only the path or mechanism of the collapse as the solvent quality becomes poorer. It does not affect the final shape of the collapsed globule.

Acknowledgment. A.K.D. acknowledges the financial assistance from the CSIR, India, JRF grant. A.K.D. would also like to acknowledge Prof. A. Swain, Department of Physics, IITB and Profs. D. V. Khakhar, V. A. Juvekar, and A. K. Suresh for useful discussions, and Dr. R. P. Thangavelu, C-MMACS, for helping in running the code on SGI Altix350 servers. H.N. acknowledges financial assistance from CSIR's Intramural Scheme (CSIR project ref no. 80(0053)/04/EMR-II). We gratefully acknowledge C-MMACS, C-DAC, and IITB for allowing the use of their computing resources. We gratefully acknowledge the valuable comments by Prof. P. Grassberger that have greatly improved this manuscript.

References and Notes

(1) Dill, K. A. *Biochemistry* **1985**, *24*, 1501–1509.
(2) Pande, V. S.; Grosberg, A. Yu.; Tanaka, O. *J. Chem. Phys.* **1997**, *107*, 5118–5124.
(3) Pande, V. S.; Rokhsar, D. S. *Proc. Natl. Acad. Sci. U.S.A.* **1998**, *95*, 1490–1494.
(4) de Gennes, P. G. *Scaling Concepts in Polymer Physics*; Cornell University Press: Ithaca, NY, 1979.
(5) Flory, P. J. *Principles of Polymer Chemistry*; Cornell University Press: Ithaca, NY, 1953.
(6) Baysal, B. M.; Karasz, F. E. *Macromol. Theory Simul.* **2003**, *12*, 627–645.
(7) Grosberg, A. Yu.; Kuznetsov, D. V. *Macromolecules* **1992**, *25*, 1970–1979.
(8) Ma, J.; Straub, J. E.; Shakhnovich, E. I. *J. Chem. Phys.* **1995**, *103*, 2615–2624.
(9) Grassberger, P.; Hegger, R. *J. Chem. Phys.* **1995**, *102*, 6881–6899.
(10) Hu, W. *J. Chem. Phys.* **1998**, *109*, 3686–3690.
(11) Timoshenko, E. G.; Kuznetsov, Yu. A.; Dawson, K. A. *Phys. Rev. E* **1998**, *57*, 6801–6814.
(12) Ganazzoli, F. *J. Chem. Phys.* **1998**, *108*, 9924–9932.
(13) Lantman, C. W.; MacKnight, W. J.; Higgins, J. S.; Peiffer, D. G.; Sinha, S. K.; Lundberg, R. D. *Macromolecules* **1988**, *21*, 1339–1343.
(14) Karal-Yllmaz, O.; Gurel, E. E.; Kayaman-Apohan, N.; Baysal, B. M.; Karasz, F. E. *Polymer* **2001**, *42*, 9433–9440.
(15) Chu, B.; Ying, Q.; Grosberg, A. Yu. *Macromolecules* **1995**, *28*, 180–189.
(16) Chu, B.; Wang, Z. *Macromolecules* **1989**, *22*, 380–383.
(17) Wu, C.; Zhou, S. *Macromolecules* **1995**, *28*, 5388–5390.
(18) Wu, C.; Zhou, S. *Macromolecules* **1995**, *28*, 8381–8387.
(19) Wu, C.; Zhou, S. *Phys. Rev. Lett.* **1996**, *77*, 3053–3055.
(20) Wu, C.; Wang, X. *Phys. Rev. Lett.* **1998**, *80*, 4092–4094.
(21) Wu, C.; Qiu, X. *Phys. Rev. Lett.* **1998**, *80*, 620–622.
(22) Zhang, G.; Winnik, F. M.; Wu, C. *Phys. Rev. Lett.* **2003**, *90*, 035506-1–035506-4.
(23) Yu, J.; Wang, Z.; Chu, B. *Macromolecules* **1992**, *25*, 1618–1620.
(24) Vasilevskaya, V. V.; Klochkov, A. A.; Lazutin, A. A.; Khalatur, P. G.; Khokhlov, A. R. *Macromolecules* **2004**, *37*, 5444–5460.
(25) Raos, G.; Allegra, G. *J. Chem. Phys.* **1997**, *107*, 6479–6490.
(26) Bastolla, U.; Frauenkron, H.; Grassberger, P. *J. Mol. Liq.* **2000**, *84*, 111–129.
(27) Pande, V. S.; Grosberg, A. Yu.; Joerg, C.; Tanaka, T. *Phys. Rev. Lett.* **1996**, *76*, 3987–3990.
(28) Bastolla, U.; Grassberger, P. *Phys. Rev. E* **2001**, *63*, 031901-1–031901-12.
(29) Garel, T.; Leibler, L.; Orland, H. *J. Phys. II* **1994**, *4*, 2139–2148.
(30) Kantor, Y.; Kardar, M. *Europhys. Lett.* **1994**, *28*, 169–174.
(31) Grassberger, P.; Hegger, R. *Europhys. Lett.* **1995**, *31*, 351–356.
(32) Hu, W.; Mathot, V. B. F.; Frenkel, D. *Macromolecules* **2003**, *36*, 2165–2175.
(33) Chanda, M. *Advanced Polymer Chemistry: A Problem Solving Guide*; Marcel Dekker: New York, 2000.
(34) Kremer, K.; Binder, K. *Comput. Phys. Rep.* **1988**, *7*, 259–310.
(35) Carmesin, I.; Kremer, K. *Macromolecules* **1988**, *21*, 2819–2823.
(36) Metropolis, N.; Rosenbluth, A. W.; Rosenbluth, M. N.; Teller, A. H.; Teller, E. *J. Chem. Phys.* **1953**, *21*, 1087–1092.
(37) Nishimura, T.; Matsumoto, M. *http://www*UTH.*math.sci.hiroshima-u.ac.jp*~m- mat/MT/emt. html, 2002.
(38) Grassberger, P. *Phys. Rev. E* **1997**, *56*, 3682–3693.
(39) Koga, T. *Eur. Phys. J. E* **2005**, *17*, 381–388.
(40) Paul, W.; Müller, M. *J. Chem. Phys.* **2001**, *115*, 630–635.
(41) Hu, W. B.; Frenkel, D. *J. Phys. Chem. B* **2006**, *110*, 3734–3737.
(42) Cowie, J. M. G. *Polymers: Chemistry and Physics of Modern Materials*; Nelson Thornes: Cheltenham, Gloucestershire, U.K., 2001.
(43) Smith, N. C.; Flemming, R. J. *J. Phys. A: Math. Gen.* **1975**, *8*, 929–937.
(44) Domb, C. *Polymer* **1974**, *15*, 259–262.
(45) Chen, T.; Changjun Peng, C.; Liu, H.; Hu, Y. *Fluid Phase Equilib.* **2005**, *233*, 73–80.
(46) Chakrabarty, K.; Seery, T. A. P.; Weiss, R. A. *Macromolecules* **1998**, *31*, 7385–7389.
(47) Tanaka, G.; Mattice, W. L. *Macromolecules* **1995**, *28*, 1049–1059.
(48) Tanaka, G.; Mattice, W. L. *Macromol. Theory Simul.* **1996**, *5*, 499–523.
(49) Šolc, K. *J. Chem. Phys.* **1971**, *55*, 335–344.

MA061017Q